Design and Prototype of a
Hovering Ornithopter Based on Dragonfly Flight

by

Theresa Guo

Submitted to the Department of
Mechanical Engineering in Partial
Fulfillment of the Requirements for the
Degree of

Bachelor of Science

at the

Massachusetts Institute of Technology
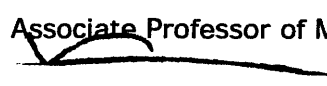
June 2007

© 2007 Theresa Guo

All rights reserved

The author hereby grants to MIT permission to reproduce and to
distribute publicly paper and electronic copies of this thesis document in
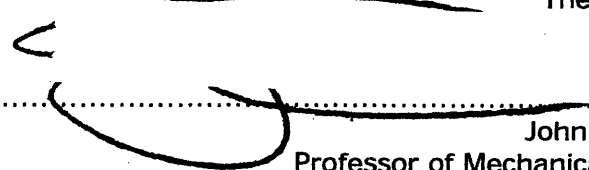whole or in part in any medium now known or hereafter created.
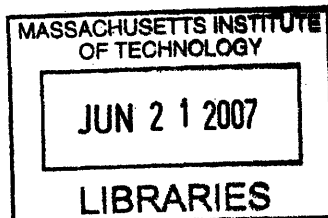
Signature of Author...
Theresa W Guo
Department of Materials Science and Engineering
May 17, 2007

Certified by ....
Anette E Hosoi
Associate Professor of Mechanical Engineering
Thesis Supervisor

Accepted by ....
John H Lienhard, V
Professor of Mechanical Engineering
Undergraduate Thesis Committee

Design and Prototype
Of a Hovering Ornithopter
Based on Dragonfly Flight

By

Theresa Guo

Submitted to the Department of Mechanical Engineering
On May 17, 2007 in partial fulfillment of
Requirements for the degree of
Bachelor of Science in Engineering
as recommended by the Department of Mechanical Engineering

Abstract

Hovering is normally achieved using a horizontal wing path to create lift; bees, wasps and helicopters use this technique. Dragonflies hover using a unique method, by flapping along an inclined stroke plane. This seems to create a higher efficiency than is possible for normal hovering. The aim of this project is to build a mechanical model to mimic the aerodynamic properties and hovering motion of dragonflies.

Through the design and evaluation of this model, we can evaluate the mechanical feasibility of reproducing the wing path using single motor control and establish whether the difference in stroke plane is advantageous for the dragonfly. By adjusting the initial angle of attack of the ornithopter's wings, we can artificially recreate varying stroke planes. A comparison of the resultant lift generated from different stroke planes showed that greater lift forces were generated with non-zero stroke planes as demonstrated in normal hovering.

Thesis Supervisor: Anette (Peko) Hosoi
Title: Associate Professor of Mechanical Engeineering

Introduction

Hovering is a unique mode of motion that requires more agility and energy than forward or upward flight. Hovering is one of the most demanding forms of flight; not only is it energy demanding, it also requires constant adjustment to maintain suspension in one place. To illustrate, one might compare hovering in air to treading water, as treading water is essentially hovering in water. For anyone who has experienced treading water, they can testify that it takes considerably more energy and concentration than swimming.

Studying hoverers provides us with two distinct advantages. First, insects with the ability to hover are often more agile, sophisticated fliers because of the demanding nature of a hovering mode of flight. Hovering experiments are also simple to conduct. It is the perfect model for a preliminary study of insect flight. Without out the complications of movement, a model of hovering only measures one force and contains minimal variation. We need not obtain a dragonfly to know how much lift it generates during hovering; this lift is simply equal and opposite to the force of gravity.

Furthermore, hovering is of interest because of its unique applications. For insects, hovering offers them the ability to hunt and catch prey in midair. For humans, hovering allows aircrafts to take off and land without requiring a landing and takeoff belt. Hovering offers a huge advantage in that there is more agility and freedom in flight; a hoverer can slow down or stop without losing lift.

Dragonflies are the earliest recorded predatory fliers, with their fossils date back 250 million years (1). The largest known insect was *Meganeura monyi*, a prehistoric dragonfly with a wingspan of up to 70 cm(2). Although it is estimated that these gargantuan
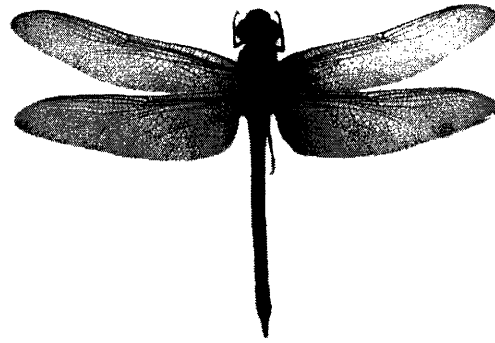

Figure 1. Anax speratus, South African dragonfly with wingspan of 120mm

insects did not have the ability to hover, its successors have not only developed the ability to hover, but also incredible maneuverability. Presently, there are dragonflies with wingspans of 120 mm (Figure 1), making them the largest hovering insects. Studying their flight may give us insights for design of both simpler and more efficient flight.

When hovering, dragonflies use a different wing path than most other insects. The most distinguishable difference is that their wing path lies on a different plane. Is dragonfly hovering more efficient than normal? The dragonfly's history and prosperity seems to suggest that this answer might be yes. This paper will specifically aim to mimic dragonfly hovering in order to find out. Normal insect hovering has been studied in the past, but not much work beyond modeling has been done to studying dragonfly hovering. We will build a robot to mimic the dragonfly's hovering wing path and evaluate it against normal hovering. We suspect that we might learn a great deal from dragonflies about the nature of hovering and perhaps mechanisms for human applications as well.

Background

Hovering is defined as flight with zero net velocity, or flying in place. For an organism to hover, it needs to provide a constant upward force equal to its weight. In forward flight, Bernoulli effects and translational lift allow flight to be achieved at reasonably high efficiencies. Hovers do not have these luxuries. Additionally, the lift needs to be generated by a cyclic motion which is able to shed any vortices created.

Figure 2. *High speed camera images of the dragonfly wing path for hovering. Note both the horizontal and vertical components of the wing path. (3)*

To these challenges, nature has provided some elegant solutions. Specifically, dragonflies have developed a distinct method of hovering. Normal hovering, as seen in bees and wasps, uses a periodic wing stroke along a horizontal plane. Helicopters also use the principal of a horizontal stroke plane to generate lift. Dragonflies are an exception to normal hovering for two reasons 1) they have an asymmetric wing path, 2) their wing path moves along an inclined plane. This paper will be concerned with studying their unique inclined wing path. Figure 2 shows high speed camera images of a hovering dragonfly to illustrate the inclined plane of the wing path.

Basic insect hovering as exhibited by bees, wasps, and fruit flies can be seen Figure 3(a). The wing travels in a periodic motion that draws a

figure eight which creates upward lift during both directions of motion. The governing Navier-Stokes equations can be expressed in elliptical coordinates (5):

$$\frac{\partial u}{\partial t} + (u \cdot \nabla u)u = -\frac{\nabla p}{\rho} + v\Delta u - \frac{dU_0}{dt} - \left[\frac{d\Omega}{dt} \times r + 2\Omega \times u + \Omega \times (\Omega \times r) \right]$$

$$\nabla \cdot u = 0$$

$$u\big|_{wing} = 0$$

Where the coordinates are in relation to the wing, u is the velocity field, p is the pressure, v is the kinematic viscosity, r is the distance from the wing axis, Ω is the rotational velocity, and U_0 is the translational velocity. Using these equations we can predict the resultant forces generated by the wing as in Figure 3.
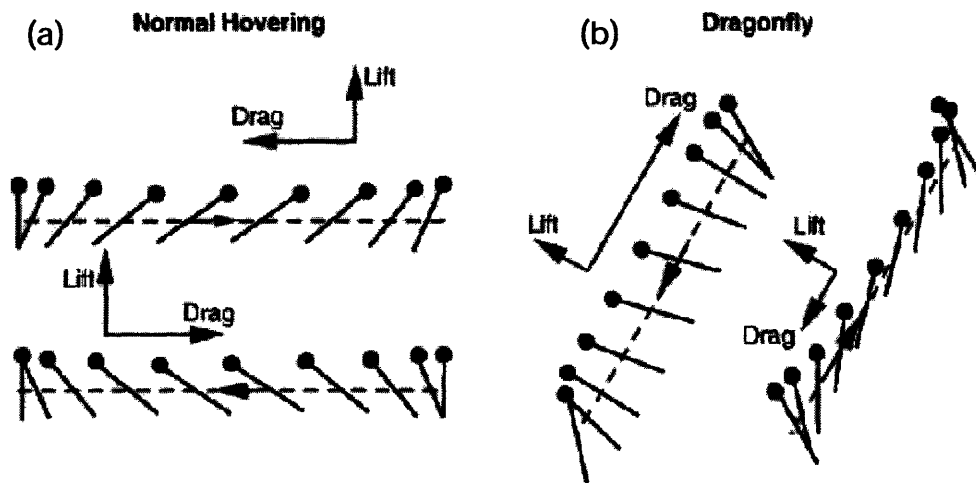

Figure 3. *Comparison of lift and drag in normal hovering to dragonfly hovering. (Wang, 2005)*

Weis-Fogh (6) observed that most hovering insects moved their wings along a horizontal plane. In principal, helicopters also use a horizontal stroke

6

plane. Conventionally, drag is associated with losses during flight because it occurs in the opposite direction of motion. But the dragonfly has an inclined stroke plane (Figure 3b). Drag forces on the down stroke of the dragonfly create an upward lift, opposite the direction of the wing motion. Because of the asymmetrical wing path, this upward lift is not cancelled out during the up stroke (4). Though there are still losses in the horizontal direction, both the lift and the drag contribute to holding up the weight of the dragonfly.

An additional difference between man-made hoverers and insects is that insects use flapping motion instead of rotary motion. Perhaps this is simply an anatomical artifact; that flapping is easier accomplished given insect anatomy as rotary motion is easier to execute given the nature of modern motors. But aerodynamically does it make a difference? According to Dickinson et. al, the flapping motion of insect flight combined with wing rotation offers three distinct advantages: "delayed stall, rotational circulation and wake capture" (7). Because of these advantages, many groups are interested in modeling and studying insect flight.

One previous robotic model of a hovering insect was created by Dickinson et al. (7). The group created a robotic fruitfly whose wings had both rotational and translational motion. We wish to exhibit these same degrees of motion in our own model. Their fruitfly incorporated three degrees of freedom which were controlled by six computer controlled stepper motors in order to simulate several different modes of flight including translational flight and hovering. While the ability to finely control a robotic insect's wing path is extremely useful for the purposes of scientific study, any

application would desire something simpler. Figure 4 shows the mechanism and the wing path created for hovering. It should be noted that the hovering wing path is like the dragonfly in that it is asymmetric, but the stroke plane is horizontal.
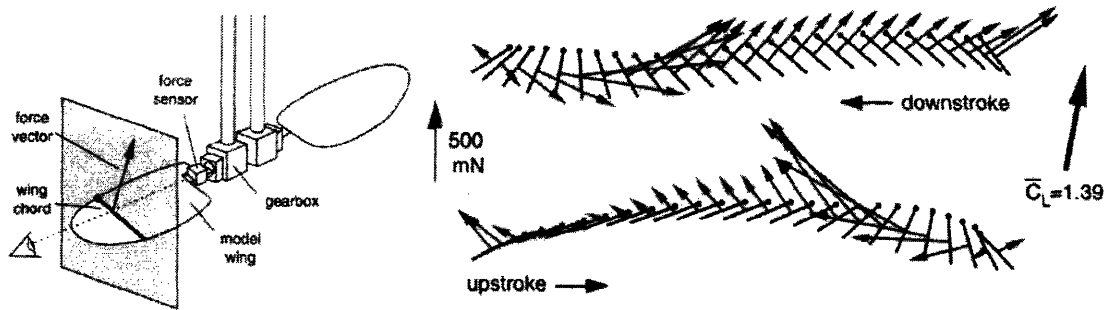

Figure 4. *Robotic fruit fly. Left shows mechanism. Right shows the asymmetrical hovering wing path. (Dickinson, 1999)*

Dickinson's group measured aerodynamic forces on the robots wings by equipping the wings with force sensors. The result, Figure 5, shows that the total lift generated seems to have peaks in lift force that could not be explained by the translational motion of the wing alone. Instead, these peaks seem to be a result of rotational motion along the axis of the wing, an aspect of hovering that is not seen in helicopters. These peaks might be explained by two phenomenon resulting from the rotational motion of the wing: (a) rotational circulation in which the net velocity of air on one side of the wing is higher creating an upward pull, similar to the effect of topspin on a ball; and (b) wake capture in which previously shed vortices offer increased force production (7).
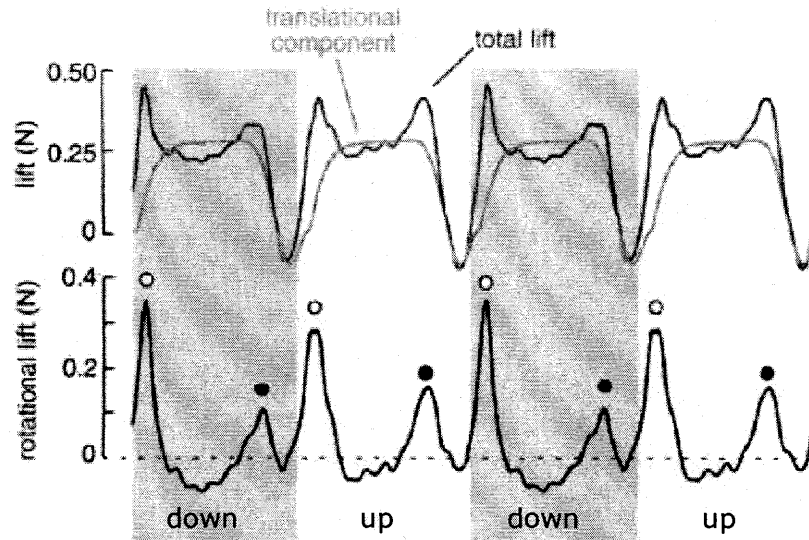
Figure 5. *Lift forces measured by Dickinson's robotic Drosophila for an asymmetrical, horizontal hovering wing path (Figure 4). Translational forces cannot account for the peaks in lift seen at the top and bottom of each stroke. Instead, these are attributed to rotational circulation (black dot) and wake capture (white dot) (7).*

Another group at Caltech (8) designed a prototype of a battery powered orinthopter with flapping wings. Their research focus was on maximizing lift through wing design which was modeled after natural fliers such as bats and dragonflies. They used MEMS technology to fabricate the wings.

Previous work has focused on varying wing patterns (7) and optimizing wing shape (8). They show us what aspects are important in gaining the advantages of insect flight. We know that rotational motion and wing shape both increase the lift forces created by insects. But does the orientation of the stroke plane, as seen in dragonfly hovering, offer an advantage as well?

We will focus on this aspect of dragonfly flight. The aim of the project is two-fold. First we wish to establish the feasibility of reproducing the wing path for dragonfly hovering using simple mechanical controls. Once we have built the robotic model, we will compare the lift generated during varying

9

stroke planes to find out what advantages a dragonfly's stroke plane might provide.

Methods

Design

First, we must study the relevant dimensionless numbers that will give us the size and time scale needed to achieve the same vortex shedding as a dragonfly. These numbers can be derived by researching existing hovering organisms' flapping frequencies, wing span and body mass.

The main constraint is the flapping frequency. Depending on the motor used, there will be a limit to flapping frequency. Using the dimensionless analysis, we can scale the robot size so that the flapping frequency we choose will be optimal for the right vortex shedding. The analysis can help us to estimate power our motor may need to provide. Additionally, these dimensionless parameters, as defined below, will also be useful in the evaluation of the robotic dragonfly performance.

Dimensionless Analysis

For various insects, we collected relevant dimensions from various sources (9-12). These dimensions were: flapping frequency, body mass, average wingspan, body length, and number of wings. The average wingspan was calculated by using the mean of wingspan ranges provided by sources. From these numbers, the approximate area of the wings was calculated by assuming a typical wing aspect ratio of 0.5. The compiled data

for various insects is shown in Table 1 arranged in descending flapping

frequency.

Insect	Flapping Freq (bps)	Mass (mg)	body length (mm)	avg wingspan (mm)	# of wings	approx. wing area (mm^2)
Honeybee	250	90	12.5	20	4	100
Housefly	190	30	6	12	4	36
Syrphis Fly (Diptera)	130	30	8	12	4	36
Bumblebee	120	3000	30	28	4	196
Hornet	100	263	45	35	4	306.25
Hummingbird Hawk Moth	85	2500	40	55	4	756.25
Sphinx Moth	26	2500	40	107.5	4	2889.0625
Aeshnidae Dragonfly	38	1100	75	115	4	3306.25

Table 1. *Complied data of dimensions and flapping frequencies of various insects, arranged in decreasing flapping frequency. Wing area was calculated with a typical wing aspect ratio of 0.5. Of these insects, bees, moths and dragonflies are able to hover.*

Of these values, those of particular interest are bees, moths and

dragonflies who are capable of hovering. Note that in general, there is a

inverse relationship between size (mass, body length and wingspan) and

flapping frequency. According to Wang et al. (3), there is an inverse

relationship between the size of the insect and optimum flapping frequency.

Figure 6 shows the relationship between flapping frequency and wingspan for

the hovering insects. Fitting a power function gives a best fit show in the

figure. Using this idea, we can obtain a rough estimate the optimal flapping

frequency for a given wingspan. Given a wingspan of 400mm, the estimated
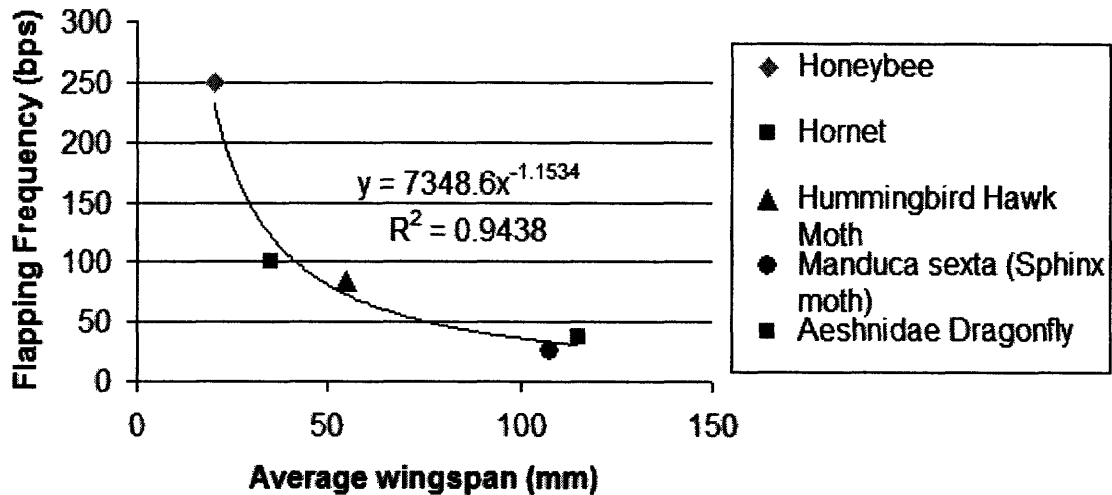
optimal flapping frequency is estimated to be 7.3 bps.

Figure 6. *The average wingspan compared to the flapping frequencies of various hovering insects. The data shows an inverse relationship in nature between frequency and wingspan. A power relationship was fitted to the points to give a rough estimate of the flapping frequency.*

Using frequency and wingspan gives only an incomplete analysis of the data. To take all factors into account, we will use dimensionless analysis. The three dimensionless numbers we will to evaluate are the efficiency (η), effective Reynolds number (Re) and the hovering coefficient (C_H).

We would like to define the efficiency by comparing the input power with the output. Although we cannot find direct measurements for the energy an insect uses to fly or hover, we can still deduce these forces using different methods.

First we wish to find how much work the insect puts into flight. The only way to directly measure this might be to take metabolic measurements of the insects during flight by measuring their respiration. Instead, we will indirectly deduce the power as the power required for the insect to move its wing through air at its given flapping frequency. The force required to push the fluid (air) through an insect's wing path is defined as

$$F_{flap} = \frac{1}{2}\rho \cdot v^2 \cdot A \tag{1}$$

where the area (A) is the total wing area and the effective velocity (v). We have defined the effective velocity as the average wing tip velocity, because in hovering, there is a zero net velocity, so true velocity would be an inappropriate measurement. The effective velocity can be calculated as the wing tip velocity:

$$v = 4 * (2.5 \cdot 0.5 \cdot l) \cdot f \tag{2}$$

According to Wang, the sweep amplitude of the wing is approximately 2.5 times the width of the wing (4). The wing width (defined by the wing length (l) and an aspect ratio of 0.5) is multiplied by this factor to find this amplitude, then multiplied by 4 to define the distance the tip travels in one beat. The tip velocity is this distance multiplied by the flapping frequency. The flapping force is multiplied the effective velocity (v) to obtain the input power.

What is the net output work achieved by the insect? In the case of hovering, there is a zero net velocity. Thus the lift generated must equal the weight of the insect and all other forces cancel. The power generated by the insect is

$$P_{lift} = m \cdot g \cdot v \tag{3}$$

Comparing these two powers gives us the effective efficiency for each insect.

The effective Reynolds (Re) number should reflect the same idea as the traditional Reynolds number, i.e. the ratio between inertia and viscous forces. Normally, the Reynolds number is defined as

$$Re = \frac{\rho \cdot v \cdot L_c}{\mu} \qquad (4)$$

with density (ρ), velocity(v), characteristic length (L_c) and viscosity (μ).

Since the fluid that insects fly in is air, we will use the density and viscosity

of air. For velocity, we will use the effective velocity as defined in equation 2.

For the characteristic length we will use the wing length (l), since it gives us

a good estimate of the size of the insect and the magnitude of its wing path.

The last dimensionless number we wish to evaluate is the hovering

coefficient (C_H). The hovering coefficient is the equivalent of a lift coefficient,

used in lift equations to estimate lift forces. But for hovering, we are using

the wing tip velocity rather than translational velocity. The coefficient is

defined as:

$$C_H = \frac{L}{\frac{1}{2} \cdot \rho \cdot v^2 \cdot A} \qquad (5)$$

The lift force (L) in the case of hovering is the weight of the insect. The

bottom of the equation is the same as what we calculated for F_{flap}. Thus, the

way we have defined our variables, the hovering coefficient is the same as

the effective efficiency. The calculated efficiencies for relevant insects are

shown in Table 2.

Insect	Frequency bps	Mass mg	Pflap mWatts	Plift mWatts	Lift Efficiencies Plift/Pflap
Honeybee	250	90	117.1875	11036.25	94.176
Hornet	100	263	123.0981	22575.26	183.3923865
Hummingbird Hawk Moth	85	2500	724.4051	286635.9	395.6845839
Aeshnidae Dragonfly	38	1100	2586.731	117891.7	45.57554403
Sphinx Moth	26	2500	591.3896	171368.4	289.7725127

Table 2. *Calculated of hovering insects based on insect dimensions and flapping frequencies.*

The calculations seem to show that, at least in nature, insects with larger mass have higher efficiencies in general. This seems to make sense since heavier insects have a greater need to be more efficient fliers. Note that dragonflies seem to be an exception to this rule. Either dragonflies are highly inefficient fliers and able consume more energy than their counterparts; or perhaps this calculation overestimates the input or flapping energy a dragonfly uses to fly. This overestimation may be explained by the dragonfly's unique stroke plane (which bees and moths do not use), since the utilization of drag to generate lift may cut down on energy loss.

Design Parameters

To select the flapping frequency and wingspan, the Reynolds number of the dragonfly was matched as closely as possible. The Reynolds number increases linearly with both the flapping frequency and wingspan. We are not aiming to match the lift coefficient because this coefficient depends on the mass of the insect. In our model, we do not have a target load that needs to be lifted. This value will be obtained during testing of the model.

We aim to make a robot with a flapping frequency of less than 300 rpm (or 5 bps). Thus by adjusting the wingspan we can try to match the Reynold's number and lift coefficient. Table 3 shows calculated wingspans for a few different flapping frequencies that will be near our operating range.

Insect	Flapping Freq (bps)	Wingspan (mm)	Reynold's number
Aeshnidae Dragonfly	*38*	*115*	*42207.45*
Scaled Models	2	503	42498.71
	3	410	42354.42
	4	355	42337.63

Table 3. *Matching Reynolds number for a range of flapping of frequencies. Ornithopter was sized for a flapping frequency of 3 bps.*

We expect the robotic dragonfly wing to have two degrees of freedom. One will be along the stroke plane, and one will be along the axis of the wing. One design challenge is to link both degrees of motion to one motor. Because both the wing rotation and flapping should have the same period, they should be able to run off the same motor control.

With single motor control, the mechanism can be more directly compared to a helicopter, the most commonly used hovering mechanism. If our ornithopter mechanism uses complex controls or multiple motors, a small increase in efficiency may not be a compelling enough reason to use the mechanism. But if the design can match the simplicity of a helicopter, while obtaining the advantages of dragonfly flight, it will be much more appealing for applications.

The constraints for design are: (1) create a wing path that mimics the wing path of a hovering dragonfly, (2) find a wingspan and frequency that will match the Reynolds number of a dragonfly, and (3) apply a feasible frequency that can be obtained by the given motor and mechanism.

To mimic the wing path, we look to the dragonfly to see what angles we need to achieve in our ornithopter's wing path in order to obtain dragonfly hovering. We will use a simplified and parameterized model of the hovering

dragonfly wing path developed by Jane Wang of Cornell. The relevant variables are the pitching angle (α), the angle of stroke plane incline (β), and the amplitude or sweep (A_0). The defined variables are show in Figure 7.
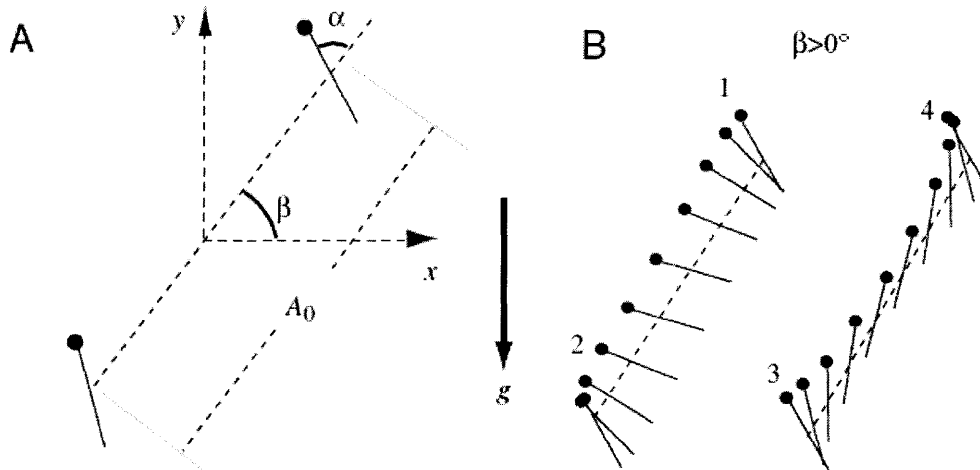

Figure 7. *(Wang, 2004) A model of the hovering dragonfly wingpath. Relevant variables are the pitching angle (a), the angle of stroke plane incline (β), and the amplitude or sweep (A₀).*

For a dragonfly, the incline angle (β) is 62.8° (as compared to 0° for normal hovering) and the initial pitching angle (α_0) is 60° (as compared to 90° for normal hovering) (4). The pitching angle has a range of 90°. According to measurements taken on real dragonflies by Wakeling and Ellington (14), during near hovering conditions the forewing achieved a sweep amplitude of 34° and the hind wing achieved one of 48°. Based on these data, we will aim for a sweep amplitude of 45°. These parameters describe the range of motion we will design our ornithopter to be able to achieve.

Overview of Ornithopter Design

Given the parameters for the size and range of motion of the ornithopter, a basic mechanism was designed to actuate flapping and rotating motion of wings. For the sake of simplicity, the dragonfly ornithopter was only designed to actuate two wings, as seen in Figure 8, instead of the four that dragonflies use.
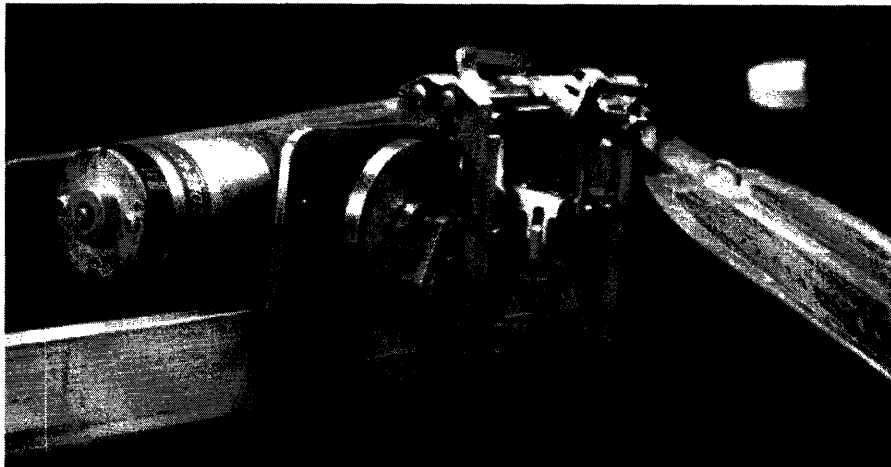

Figure 8. *Photograph of designed robotic ornithopter model. The actuation mechanism is connected to the mount, wings, motor, and lift measurement beam.*

The first component of the ornithopter design is the translation of the driving motor's rotational motion to a flapping motion. The actuation of flapping is detailed in Figure 9. As the motor drives, the lever (A) oscillates vertically. This lever pushes up parts connected to both wings (B). This motion causes the parts in B to pivot around the main axis (C), creating a flapping motion. One full cycle of the motor driven wheel produces a flapping motion with amplitude of 45°.
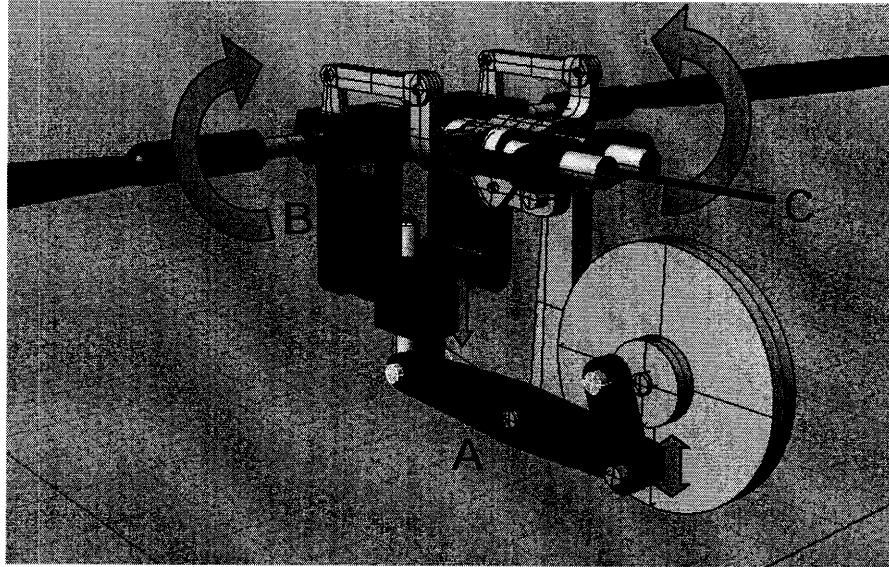
18

Figure 9. *Flapping motion actuation. Parts involved in the producing the flapping motion of the ornithopter are highlighted in purple. The lever arm (A) pushes both wings (B) to pivot around the main axis (C) to produce a flapping motion.*

The rotational motion is actuated by the other side of the motor driven wheel, detailed in Figure 11. Creating the rotating motion of flapping wings is not a trivial thing. The dragonfly's wing does not rotate in full circles as it hovers, instead it flips back and forth oscillating between a minimum and maximum pitching angle. We must transform the motor's motion from full circle rotation to an oscillating tilt. The solution proposed is based on a design model used by Chan for modeling snails an asymmetrical track is used to achieve the desired motion (13). The track used is shown in Figure 10. It features two radii and a transitional track. The small radius is 0.3125" and the large is 0.6875". A pin in an arm (D in Figure 6) is placed in the track, as shown in Figure 6. During the rotation of the wheel, the difference in radius translates to a difference height of the pin (or a distance
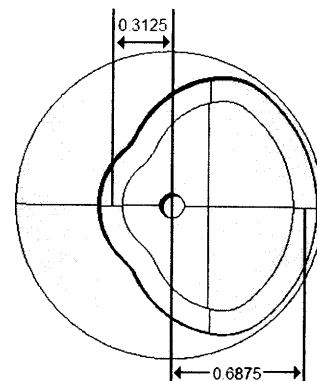

Figure 10. Track for rotational actuation with two radii.

from the motor shaft). When the pin is reaches the small radius, the one

side of the arm (D) is lifted. The arm pivots and pushes the back on pieces

connected to both wings (E) which slide back along the main axes (C in

Figure 9). This backward motion causes the small arm (F) to pivot and

rotate the wing (G). The backward motion causes the wings to tilt back.

Inversely, when the pin reaches the large radius, the parts (E) slide forward

along the axis to create forward rotation. The range of the pitching angle

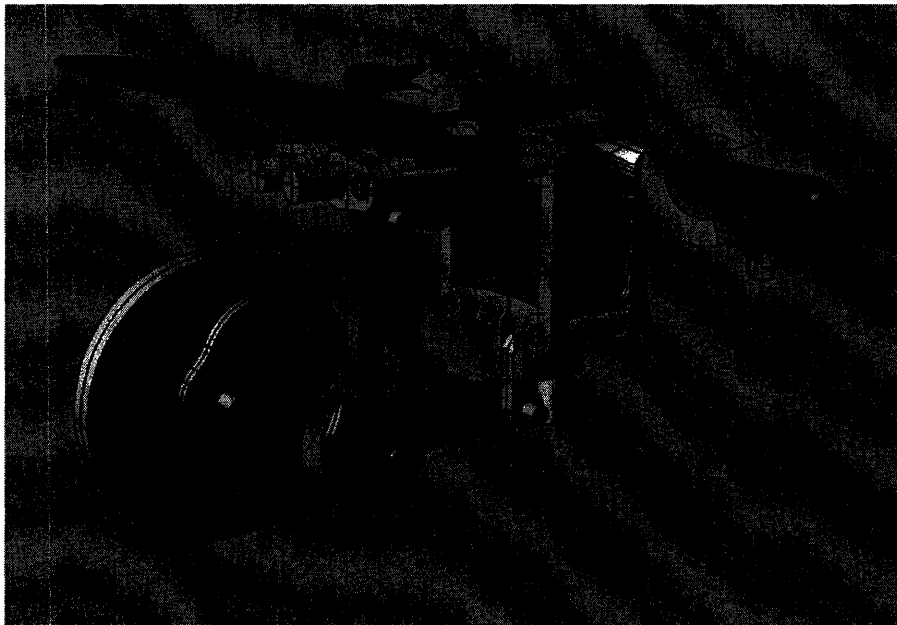achieved by the ornithopter is 90°.

Figure 11. *Rotational motion actuation. Parts in green are involved in producing the change in pitching angle in conjunction with flapping.*

The coordination of the translational flapping and the rotational

movement is achieved by actuating both movements with the same wheel.

The flapping motion is actuated on the side of the wheel opposite the motor

so that the motor shaft will not restrict movement of lever (A). We also

coordinate both motions by pinning the rotor of the flapping motion in a way so that the wing changes angles at the top and bottom of its wing path. This means that the tilting arm (D) should transition to a different radius when the flapping lever (A) reaches its minimum and maximum. This is the configuration suggested by Dickinson in order to achieve an upward lift from rotational circulation (7).

Wings

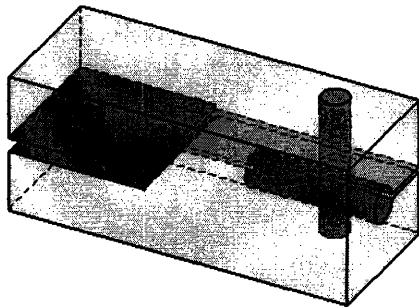The most important aspect of the wing design is the attachment of the wings to the ornithopter. In order to test the difference between stroke planes, we must be able to adjust either the stroke plane or the initial angle of attack. In our design, the wings were attached so that the angle of the wing could be adjusted.

Figure 12. *Wing mount to allow angle adjustment. A cap screw in pink hole holds the wing in on shaft (grey) with a friction fit.*

As shown in Figures 9 and 11, the wings were attached to an 1/8" steel pin. Using the polycarbonate mount shown in Figure 12, the wing is loosely fitted onto the steel shaft, then tightened to achieve a friction fit. The shaft fits into the gray hole while a cap screw in the pink hole causes the thin (light blue) slot to close and tighten the shaft around the steel shaft. The wing itself is attached with pins inside the dark blue slot.

Materials

To optimize the ornithopter, we need to (a) minimize weight of moving parts and (b) reduce friction. For these reasons, we chose aluminum as a base material. Aluminum is light, but strong enough that parts will not deform when the ornithopter is run. Since parts are moving along axes, correct alignment is essential for smooth motion; it will also reduce the torque required from the motor. To further reduce weight, material was removed from moving parts wherever possible; an example is shown in Figure 13A. To reduce friction on moving junctions, brass inserts were created to line holes for fluid motion, as show in Figure 13B. For more complex parts with thin walls, the entire part was made from brass (13C). The part shown in Figure 13C did not need to be lifted by the flapping mechanism, so a heavier material did not significantly increase required torque. For axes and connections, steel pins were used to reduce friction.
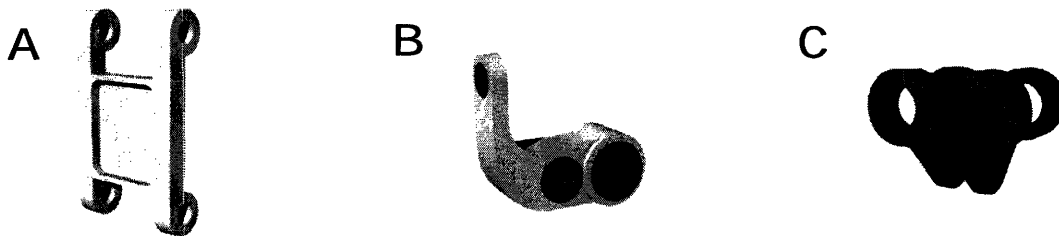

Figure 13. *Example of parts. To reduce weight, material was removed wherever possible (A) without compromise the strength of the part. To reduce friction, brass inserts were created for moving parts (B). Some parts were made entirely from brass (C).*

Materials used for the wing were also chosen to minimize weight while maintaining enough stiffness to produce the lift force desired. Because the wings reach the farthest from the axis of actuation, they were a large source of torque. Reducing the weight of the wing significantly reduced the torque

required to actuate the ornithopter. Using polycarbonate sheet of 0.04"

thickness, an outline of the wing shape was cut out, with an average width of

0.25". A strip of polycarbonate was left through

the center axis of each wing as a backbone to

help the wing maintain stiffness. LDPE wrap,

0.001" thickness, was affixed to the

polycarbonate outline to provide skin for the

wings. By using LDPE wrap instead of solid

polycarbonate wings, each wing was cut down to

less than a third of its original weight to a final

mass of 3.5 grams.

Figure 14. *Close up image of wing and attachment.*

Evaluation of design

After assembling the main mechanism, several motors were tested to

see if they could provide the power needed to actuate the ornithopter. The

aerodynamic energy needed to move the wings through the air at the given

frequency was negligible compared to the energy required to move the wings

and heavy metal parts of the robot. Thus, the power and torque required of

the motor could not be estimated by the insect models.

Because there was not simple way to test the torque required to drive

our robot, no motor was specifically chosen. Instead, several high power

motors were tested until one was able to run the robot at a reasonable speed

(near 2-3 bps). The motor selected was a 24V DC Globe motor (Part #

405A6103-3).

Using this motor, with a power of 10 V and 0.5 A, the ornithopter ran at 2.66 bps with a wingspan of 412mm. These dimensions give a Reynolds number of near 30,000. Though this number is not exactly the Reynold's number of the dragonfly (42,000) (see Table 3), it is still near the same order of magnitude.

Evaluating Lift

Accurate testing methods are essential to the evaluation of the model. At low flapping frequencies, we do not expect to be able to create enough lift in the wings to actually make the apparatus hover (or we do not expect the robot's weight to be on the order of an insect). The ornithopter, including the mount and motor, has a mass of nearly 450 grams, much greater than the 1.1 gram mass of a dragonfly. Instead of observing flight and acceleration, we will mount the ornithopter onto a measurement device that will not require the ornithopter to lift its own weight. This measurement technique must be sensitive enough to accurately measure lift forces of 10 to 20 mN, near magnitude of force generated by a dragonfly.

The measurement solution used was a simple balance scale. The ornithopter was secured at one end of a stiff aluminum beam, and a counterweight was secured on the opposite side. The fulcrum of the scale was mounted on to a tripod with ball bearings so there would be no restriction in the measurement of lift.

Because the ornithopter was secured to end of the aluminum beam, only lift in the vertical direction can be measured. Pure hovering would only

create lift in vertical direction. But, we do not know if we have achieved pure hovering or not. Additionally, by adjusting the attack angle, we are effectively changing the stroke plane, and the lift force generated in the varied stroke planes will have both a horizontal and vertical component.

To measure the horizontal component of the lift, we created a second mounting configuration for the ornithopter, flipped 90° counterclockwise on the balance scale. In this configuration, any horizontal lift force will be measured as vertical lift, and can be recorded with the same balance scale. The two force components are combined to obtain a resultant lift force and effective stroke plane.

Measurement

To measure displacement, a ruler was placed behind the ornithopter. A piece of pointed sheet brass was affixed to the ornithopter to point and give a single point reference to the ruler. Using this measure, the displacement of the ornithopter could be measured within 1-2 mm.

Additionally, each test was recorded on a video camera. The camera was used to verify displacements recorded by eye. More importantly, the camera recorded the beating of the ornithopter wing to give a measure of the flapping frequency for each trial. The frequency was calculated by counting the number of beats in a 15 second span to allow for any irregularities in beating to even out.

Calibration

Once the displacement has been recorded, it needs to be converted to a lift force. Objects of known mass were placed on the ornithopter near the wings (where the lift force would be generated) and the displacement was recorded. This calibration was performed using weighed items of between 1-6 grams, the range we expect our lift forces to fall.

The sensitivity of the scale was dependent on the positioning of the counterweight and its weight distribution; the sensitivity was also dependent on the weight distribution of the robot, but this parameter could not be adjusted as easily. For this reason, each time the setup was adjusted, a new calibration was required. And the apparatus was set up to be sensitive enough to strongly detect a change in at least 1 gram.

To extrapolate the lift force generated by the ornithopter, a few approximations were made. First, the displacement was assumed to be linear, with zero displacement for zero force. This assumption was found to be valid as the R^2 values of the linear regression lines were 0.94 and 0.99. We assume that upward and downward force both follow the same linear pattern. Additionally, because the ornithopter is mounted to a rotating beam, a lift force does not move it strictly vertical, but also along a slight arc; because we only achieve small angles, this effect was also assumed to be negligible. The calibration constant for horizontal tests was 0.209 cm/mN and 0.1451 cm/mN.

Results

After calibration, horizontal and vertical displacements were recorded for 4 initial pitching angles or attack angle (a_0 in Figure 7). Using calibration equations, the displacements were converted to lift forces and recorded in Table 4. The range of the pitching angle is 90°, so the angle on the downstroke is 45° less than the a_0 (with respect to horizontal) and the angle on the upstroke is 45° more. An initial angle of attack of 0° was reflective of normal hovering. It had an attack angle of -45° on the downstroke and +45° on the upstroke. In the plane of the stroke, forces effectively cancel (as shown in normal hovering in Figure 3), thus little force was measured in the y direction; instead most of the force was measured in the x direction. An initial attack angle of 45° put the wing horizontal (0°) during the downstroke and vertical (90°) during the upstroke to produce the maximum vertical lift. But, because applied power, frequency and wing shape were held consistent for each trial, the resultant force was nearly constant.

Initial attack angle	Y (mN)	X (mN)	Total force (mN)
0	1.44	29.634	29.67
15	6.22	32.39	32.98
30	25.359	24.12	35.00
45	31.58	6.89	32.32

Table 4. *Lift forces measured for various initial angles of attack. The lift force measured both when the ornithopter was placed upright in the horizontal position (y) as shown in Figure 8, and when it was placed on its side in the vertical position (x).*

For analysis, the measured forces made dimensionless by dividing by a standardized force, using the flapping or aerodynamic force (Equation 1). The variables were defined as the density of air (ρ), wing tip velocity (v)

based on a 45° sweep amplitude, and area (A) was defined as wing length

squared. The wing tip velocity was dependent on the flapping frequency, so

varied for each trial.

The effective stroke angle was calculated by taking the inverse tangent

of the ratio between the y and x lift forces. Note that the effective stroke

plane angle for the initial pitching angle of 0° has an effective stroke plane of

nearly 0°, as expected for normal hovering. We did not achieve any stroke

plane angles that were exactly that of a dragonfly (62.8°), but the stroke

plane angle closest to a dragonfly achieved the highest resultant force

(Figure 14).

Effective stroke plane angle	Dimensionless y lift force	Dimensionless x lift force	Dimensionless lift force
2.77	18.8645	389.468	389.92
11.35	81.746	407.191	415.32
47.88	318.785	288.256	429.79
80.35	462.22	78.554	468.85

Table 5. *Dimensionless representation of results. Measured forces were divided by the calculated flapping or aerodynamic force to make values dimensionless. The effective stroke plane was calculated by taking the inverse tangent of the ratio of y and x lift forces.*
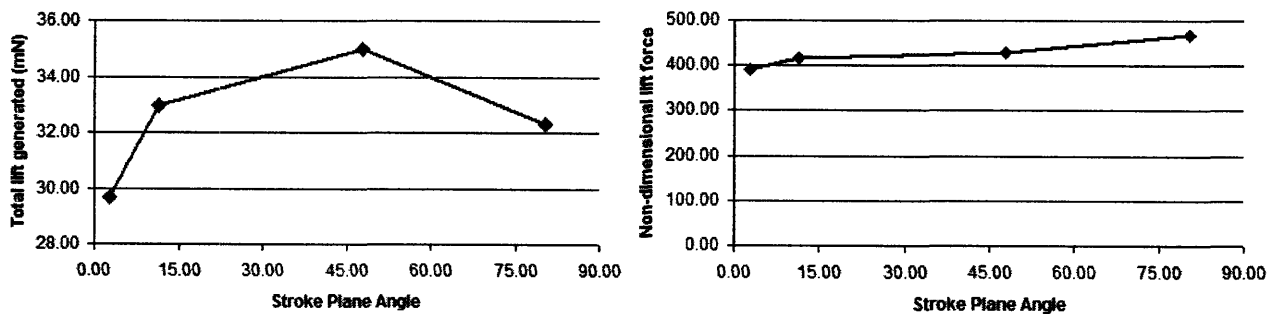

Figure 15. *Stroke plane angle compared to total generated lift. Left graph shows actual generated lift; right graph shows dimensionless lift force. Similar trends are shown, but data for 80° stroke plane was taken at a slightly lower frequency, so non dimensional result was higher.*

Discussion

28

Though the graph (Figure 15) of the generated force showed a peak at a stroke plane of 47°, the dimensionless results show us that this may not be a true maximum. Because the data points for the stroke plane of 80° happened to be at a slightly lower frequency, the generated lift was artificially low.

Even though a specific trend has not presented itself in the data, it is clear that the lift generated in normal hovering (0° initial pitching angle) was the lowest. With limited data, we are unable to establish an optimum stroke plane angle, if such an optimum exists. Yet, we can argue that the stroke plane does indeed effect the lift flapping wings are able to generate from the same amount of power.

Although the differences in lift force for varying stroke plane do not appear to be graphically dramatic, they are differences of 5-20% that cannot be entirely explained only through experimental error. The frequency was one potential source of error, even when measured over a span of 15 seconds, as beat counting was hard to standardize. Even so, a miscount of ± 1 beats would generate an average error propagation of 5.29% error in frequency. Another potential source of error was in measurement of displacement. The displacement could be read with a resolution of 1 mm. The total propagated error in the dimensionless force calculation is 8.45%. Although this is significant error, the differences between measured between stroke planes exceeded the error. Thus we can confidently assert that the generated lift of the ornithopter is affected by the stroke plane in a way that favors dragonfly hovering over normal hovering.

Now that an ornithopter and measurement scheme have been designed and built, there is much potential for future work. With a way to establish higher resolution for the initial pitching angle, one could take more data to verify a trend in generated lift force for varying stroke planes and specifically match the stroke plane of the dragonfly. By varying the power, or wing lengths, a dimensionless generated force could be compared to the effective Reynolds number to find an optimal Reynolds number range; perhaps the dragonfly already operates under this range? Another next step to take is to take into account the other unique feature of dragonfly hovering, the asymmetrical wing path. By designing new tracks for the rotating wheel, one could achieve a variety of wing paths that might be even more reflective of dragonfly hovering.

Acknowledgements

Sources

(1)   Griffith, Vive. "Aerial Acrobats." Feature Story, University of Austin Texas.
(http://www.utexas.edu/features/2006/dragonflies/index.html), 2006.

(2)   "Giant Dragonflies." Transvaal Museum,
(http://www.nfi.org.za/inverts/BIG12/dragonfly.html)

(3)   Wang, JZ. "Dissecting Insect Flight." Annu. Rev. fluid Mech., 37, (2005): 183-210.

(4)   Wang, JZ. "The role of drag in insect hovering." Journal of Experimental Biology, 207, (2004): 4147-4155.

(5)   Wang, JZ. "Two Dimensional Mechanisms for Insect Hovering." Physical Review Letters, 85(10), (2000): 2216-2219.

(6)   Weis-Fogh, T. "Quick estimates of flight fitness in hovering animals, including novel mechanisms for lift production." Journal of Experimental Biology, 59, (1973): 169-230.

(7)   Dickinson, MH, Lehmann FO, Sane, SP. "Wing Rotation and the Basis of Insect Flight." Science, 284, (1999):1954-1960.

(8)   Pornsin-sirirak, TN, et al. "MEMS Wing Technology for a Battery-powered Ornithopter." IEEE (2000): 799-804.

(9)   K-8 Aeronautics Internet Text, 1997, Cislunar Aerospace, Inc. (http://wings.avkids.com/Books/Animals/instructor/insects-02.html)

(10)   Western Exterminator Co. Website, 2003, (http://www.west-ext.com/honey_bee.html)

(11)   Ramel, Gordon. *Dragonflies* (*Odonata*), Wonderful World of Insects. (2007) Earth-Life Web Productions, (http://www.earthlife.net/insects/odonata.html)

(12)   Horbrand, Thomas. *Mandduca sexta sexta*, Giant Moths (Saturniidae) of Prince Edward Island. (http://www.silkmoths.bizland.com)

(13)   Chan et al. "Mechanical Devices for Snail-like Locomotion," Journal of Intelligent Material Systems and Structures, (2007), Vol. 18: 2, 111-116.

(14)   Wakeling, JM and Ellington, CP. "Dragonfly Flight: II. Velocities, Accelerations, and Kinematics of Flapping Flight," Journal of Experimental Biology, 200, (1997), 557-582.